Electrical Power and Energy Systems 103 (2018) 421–430

Contents lists available at ScienceDirect

Electrical Power and Energy Systems

journal homepage: www.elsevier.com/locate/ijepes

An optimal reactive power control method for distribution network with soft normally-open points and controlled air-conditioning loads

Qianggang Wang[a,*], Jianquan Liao[a], Yu Su[a], Chao Lei[b], Tao Wang[c], Niancheng Zhou[a]

[a] State Key Laboratory of Power Transmission Equipment and System Safety and New Technology, Chongqing University, Chongqing 400044, China
[b] State Grid Sichuan Electric Power Company Tianfu New Area Power Supply Company, Chengdu 610000, China
[c] KLA-Tencor, Singapore 639798, Singapore

ARTICLE INFO

Keywords:
Distribution network
Soft normally-open point
Air-conditioning load
Voltage control
Starting voltage constraint

ABSTRACT

The paper proposes an optimal reactive power control method for distribution systems with soft normally-open points (SNOP) and considering the direct load control (DLC) of thermostatically controlled air-conditioning loads. The starting voltage constraints of aggregate air-conditioning loads connected into a distribution network is studied according to the direct control mode and the starting characteristic of air-conditioning load. Using the flexible regulating capacity of power flow of SNOP, an optimal model of reactive power flow for distribution systems with SNOP is established to meet the voltage quality of sensitive loads and the starting requirements of aggregate air-conditioning loads. In the model, the load balancing commands of different DLC aggregators, the on/off status of thermostatically controlled air conditioner, the power regulating command of SNOP, the voltage adjusting and reactive power compensation devices are comprehensively controlled in the constraints of reduction balance and starting voltage of air-conditioning loads, as well as the conventional network and voltage constraints. And a multi-objective functions are developed for the objectives of solving the low-voltage problems, minimizing the comfort impacts on users of air-conditioning and minimizing the active power loss of distribution systems. Finally, the simulation results of a practical 53-bus 10 kV distribution system demonstrate the accuracy and effectiveness of the proposed method.

1. Introduction

Load demands of distribution systems usually maintains at a high level in the summer and the winter, because of seasonal temperatures in a longtime. Because of the heavy load condition of distribution networks, the low-voltage problems are widely occurring and influencing the power supplying quality of consumers [1]. For urban areas, the maximum air-conditioning loads can reach 30–40% of the peak load in a day [2,3]. For example, it is estimated that air-conditioning loads are in a proportion of 43% in 2016 and shows an increasing trend in recent years in Chengdu, China. Thus, the demand-side management (DSM) of aggregate air-conditioning loads is introduced to encourage clients to decrease the power usage during peak load periods by Electric Power Research Institute (EPRI) [4]. There are many methods to engage clients in DSM, including pricing-based approaches (time-of-use pricing, critical-peak pricing, peak-time rebate, and real-time pricing) as well as direct load control (DLC) [5–8]. The DLC programs are mostly applied when the system is in an extreme event (such as high production costs, low system reliability) to provide the ability of power balance and frequency regulation by shedding partial loads. And the air-conditioning loads have a large amount of capacity for heat storage, which have potentials for power load regulations by direct load control (DLC) conducted by electric power companies [8]. To alleviate the low-voltage problems in the distribution network in the heavy load conditions, the DLC of thermostatically controlled air-conditioning loads is an effective measure for shifting and averting the peak load [9–11] when a reasonable cycle control is implemented for the air-conditioning loads in the power scheduling procedure.

Active control of power flows and voltages by power electronic device is an alternative measure to address the low-voltage problems of distribution networks [12,13]. Soft normally-open points (SNOP) are power electronic devices replacing normally-open switches connecting the adjacent feeders. The concept of SNOP is proposed in [14] to enhance the flexibility of current distribution networks by little equipment or infrastructure upgrades. There are three types of topologies can be adopted for the SNOP, including back-to-back voltage source converter (VSC), unified power flow controller, and static series synchronous compensator [15–18]. The control modes of SNOP employed back-to-back VSC are analyzed during the normal operation condition and the fault isolation and supply restoration under grid fault condition

* Corresponding author.
E-mail addresses: yitagou@cqu.edu.cn (Q. Wang), Tao.Wang@kla-tencor.com (T. Wang), cee_nczhou@cqu.edu.cn (N. Zhou).

https://doi.org/10.1016/j.ijepes.2018.06.027
Received 26 December 2017; Received in revised form 8 May 2018; Accepted 8 June 2018
0142-0615/ © 2018 Published by Elsevier Ltd.

in [16]. To make use of the potential capability of SNOP, the operational benefits of a distribution network with SNOP is quantified in [17], and then an optimal method to determine the siting and sizing of SNOP is presented in [18]. The SNOP is able to improve the controllability of distribution system by reconfiguring the network and regulate active and reactive power flows between feeders, and the reactive powers at both sides of SNOP are regulated independently. Due to the bus voltage of distribution network can be changed by controlling the active and reactive power flows, the SNOP is applied to increase the penetration of distributed generation in [19,20]. The SNOP can also isolate the voltage disturbance on one feeder from the other feeder [21], thus the operation strategy of SNOP plays a key role to enhance the security and efficiency of distribution network [20]. The existing studies have investigated the optimal operation of SNOP in distribution networks. However, the operating strategy of the network both with SNOP and DLC has not been studied. The coordination of SNOP and DLC is more effective to enhance the voltage quality of distribution feeders with the heavy air-conditioning loads.

In the cycle control of DLC, the air-conditioning loads have to be started up or shut down back and forth, when the room temperature goes up and down. In particular, the high reactive power consumption of air conditioners in starting procedure may cause voltage collapse of the network. If the voltage does not satisfy the starting requirement, these air-conditioning loads cannot be started up in this cycle [22,23]. By the active power regulation and reactive power compensation of SNOP, the starting voltage constraint of air conditioners can be effectively relieved in the cycle control. The introduction of SNOP can guarantee the security of the cycle control of air-conditioning loads in distribution networks, and also can improve the load balancing level between different distribution feeders. In [9,10], the cycle control of air-conditioning loads is adopted to mitigate the unbalance between power supply and demand in the presence of renewable power generation, and the distributed model predictive control scheme is proposed to control the aggregate air-conditioning loads for the ancillary load balancing service in [24]. The Refs. [16,25–27] indicate that the DLC of aggregate loads and the power control of SNOP are both the distributed flexible resources in smart distribution networks, while the existing studies do not develop the utilization potential of SNOP to support the voltage control of distribution network with the DLC air-conditioning loads. In addition, the critical starting voltage of air-conditioning loads is a key indicator to assess their starting processes during the cycle control [28]. The critical starting voltage should be incorporated into the DLC of air-conditioning loads to determine whether the air conditioners are successfully started up.

To satisfy the voltage control requirements of distribution network with DLC and SNOP in consideration of the starting processes of air-conditioning loads, this paper proposes an analytical method to calculate the critical starting voltage of aggregate air-conditioning loads according to DLC control mode and the starting voltage characteristic. In the constraints of voltage quality of sensitive loads and starting voltage of air-conditioning loads, an optimal reactive power control method for a distribution system is established by using SNOP and the other voltage adjusting and reactive power compensation devices. The method is a collaborative integrated solution for demand responses and voltage quality enhancements. The proposed technique is verified by simulation results of a practical 53-bus 10 kV distribution system.

2. Critical starting voltage of air conditioning load

For the resource of demand response of air-conditioning loads with heat storage capacity, the DLC cycle control can be applied to provide load balancing service. In Fig. 1(a), the DLC aggregate has n controlled air-conditioning loads (D_1, D_2, …, D_n), and the aggregate is in charge of the loads in a same feeder. According to the dispatching commands of an electric power company, the aggregate determine the on/off status of air conditioner in the DLC cycle control for load shedding [11]. Fig. 1(b) shows the cycle control of air conditioners when $n = 10$, which can be numbered from 1 to 10 (corresponding to the 1st to 10th air conditioners) in the small square box. If the room temperature drops to the lower setting $T_{\min}$, the relevant air conditioner will be off status which is the gray box. When the room temperature rises to $T_{\max}$, the air conditioner needs to be started up corresponding to the on status of white box.

In a control cycle from 0 to t_{on}, the on status duration of an air conditioner is t_{on}-t_{off}. The starting characteristic of air conditioner can be represented by an induction motor [23,28], in which the starting electromagnetic torque is proportional to the square of the applied voltage. When the supply voltage is connected to the stator of an induction motor, a rotating magnetic field is produced, and the rotor starts rotating. During the starting process, the rotor speed rises from zero to the rated speed due to the driving electromagnetic torque is larger than the braking mechanical torque, and then the induction motor will operate at an equilibrium point that the electromagnetic torque is equal to the mechanical torque [29]. At the starting time of air conditioner, the rotor slip is unity, and the starting current is very large. The corresponding reactive power is closed to 4–6 times the rated power of air-conditioning loads, which will result in a sharp voltage drop at the connected point of air conditioners. The critical starting voltage is the minimum condition of the starting of air conditioners. Once the terminal voltage is lower than the critical starting voltage, there are no equilibrium points between the electromagnetic torque and the mechanical torque. And then the electromagnetic torque is always lower than the mechanical torque, so that the speed of air conditioner cannot be accelerated to the rated speed, and the air-conditioning load will fail to start. When the terminal voltage is larger than the critical starting voltage, the motor speed can be accelerated for the successful startup of air-conditioning load. Thus the DLC cycle control of air-conditioning loads will keep working when the terminal voltage satisfies the minimum condition of the starting of air conditioners; otherwise the DLC will fail. The critical starting voltage has to be determined to judge whether the system voltage meeting the starting conditions of air-conditioning loads.

The power demand during the starting of air conditioner is mainly from a compressor which has the similar dynamic voltage characteristic with induction motor. Fig. 2 shows the electromagnetic and mechanical torques-speed curves of an air-conditioning load where the parameters are in [28]. When the starting voltage is high enough, there are intersection points (stable equilibrium points) between the curves of electromagnetic torque T_e and mechanical torque T_m. In this case, the motor speed ω_r can be accelerated to the equilibrium point after the starting process [29]. If the terminal voltage is lower than the critical starting voltage, there are no intersection points between the curves of T_e and T_m. The mechanical torque is still higher than the electromagnetic torque under different speeds, so the motor cannot run steadily on the normal equilibrium state.

The mechanical torque T_m of air-conditioning load is proportional to the square of the rotor speed ω_r [23], and the electromagnetic torque T_e is in terms of the rotor speed ω_r and the terminal voltage U in Fig. 2. The critical starting voltage U_{cr} can be got by $T_e(\omega_{rmax}, U_{cr}) = T_m(\omega_{rmax})$, where ω_{rmax} is the rotor speed corresponding to the maximum electromagnetic torque. For the case in consideration of the network impedance, $U_{cr} = 0.95$ pu. However, there are still stable equilibrium points between T_e and T_m when $U = 0.95$ pu in the case without the network impedance that meets the starting requirement of air conditioner. Thus, it is needed to consider the network impedance to determine the critical starting voltage.

Using the equivalent circuit of induction motor as an air-conditioning load, the equivalent circuit of an aggregator with n controlled air-conditioning loads is shown in Fig. 3. U_i is the voltage at the connecting point of aggregator; R_k and X_k ($k = 1, 2, …, n$) are the line resistance and reactance; R_{sk}, R_{rk}, X_{sk} and X_{rk} are stator-side and rotor-side resistance and reactance of k^{th} air-conditioning load; X_{mk} is the

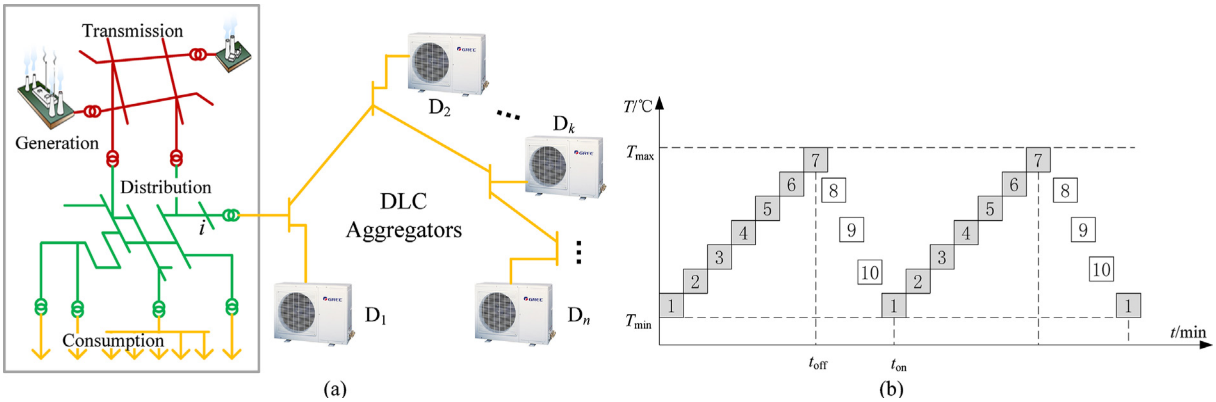

Fig. 1. Cycle control of air-conditioning loads: (a) network structure of a load aggregator and (b) cycle control modes.

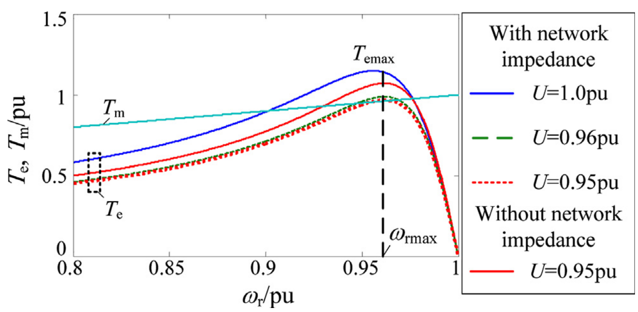

Fig. 2. Electromagnetic and mechanical torques of an air-conditioning load.

magnetizing reactance; $s_k = (\omega_s - \omega_{rk})/\omega_s$ is the rotor slip where ω_s is the mains angular frequency, ω_{rk} is the rotor angular speed. To achieve the Thevenin voltage and impedance from the connecting point of k^{th} load to the network, it is assumed that the k^{th} air-conditioning load is not connected (the node k is open circuit). And then the impedance matrix $\boldsymbol{Z}$ of the residual network can be got by the impedance parameters and the known rotor slips of the other air-conditioning loads. The diagonal element Z_{kk} of $\boldsymbol{Z}$ is the Thevenin equivalent impedance of node k [30]. Since the voltage source U_i is the only source in Fig. 3, the Thevenin voltage at the node k is,

$$U_{ock} = \frac{Z_{kk} U_i}{\sqrt{R_1^2 + X_1^2}} \tag{1}$$

where Z_{k1} is the element of the impedance matrix $\boldsymbol{Z}$, and the $\boldsymbol{Z}$ is formed by the line impedances, the impedances and rotor slips of air-conditioning loads except the k^{th} air-conditioning load. The rotor speeds of maximum T_e are same under different terminal voltages (Fig. 2) since T_e is proportional to the square of terminal voltage.

The rotor current equations of the network when $U_i = 1$ pu can be obtained, which corresponds to $T_{ek} - T_{mk} = 0 (k = 1, 2, \ldots, n)$ of n loads. The equations are solved by Newton-Raphson method to obtain rotor currents and rotor slips of air-conditioning loads at equilibrium points [29]. Substituting the rotor slips into $\boldsymbol{Z}$, the Thevenin voltage and impedance at node k can be obtained. Fig. 4(a) shows the Thevenin equivalent circuit of k^{th} air-conditioning load, and Fig. 4(b) is the simplified equivalent circuit of Fig. 4(a). The equivalent voltage and impedance are modified as,

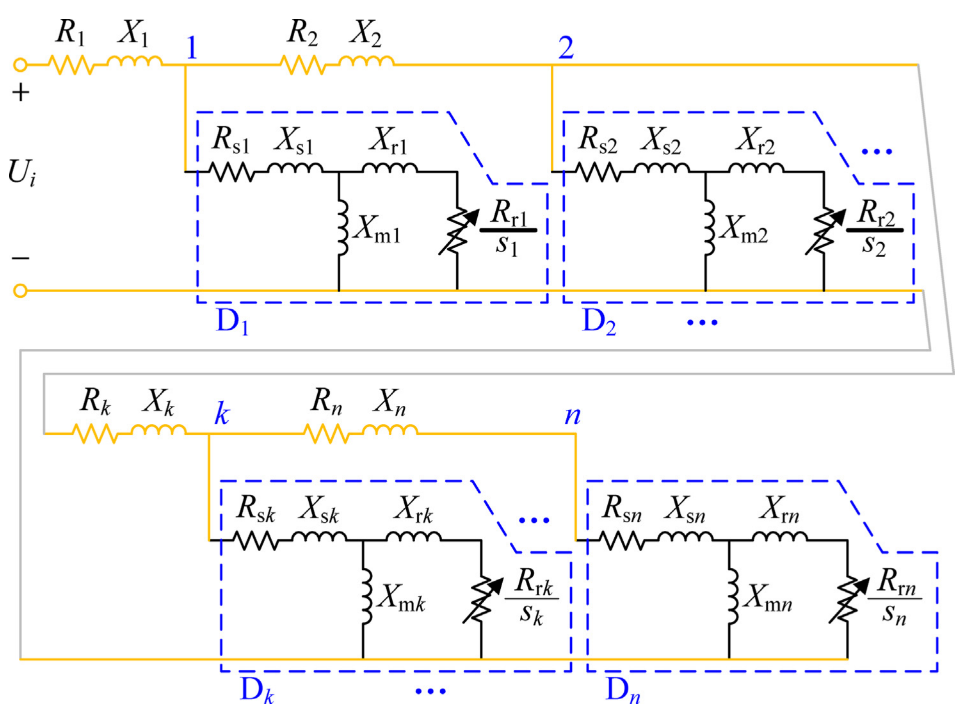

Fig. 3. Equivalent circuit of an aggregator with air-conditioning loads.

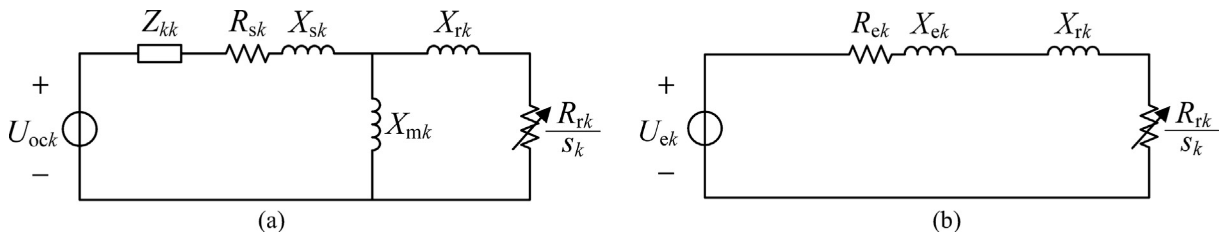

Fig. 4. Equivalent circuits of k$^{\text{th}}$ air-conditioning load: (a) Thevenin equivalent circuit, (b) simplified circuit.

$$U_{ek} = \frac{jX_{mk}U_{ock}}{R_{sk} + j(X_{sk} + X_{mk}) + Z_{kk}} \tag{2}$$

$$R_{ek} + jX_{ek} = \frac{jX_{mk}(R_{sk} + jX_{sk} + Z_{kk})}{R_{sk} + j(X_{sk} + X_{mk}) + Z_{kk}}. \tag{3}$$

From the simplified equivalent circuit in Fig. 4(b), the electromagnetic torque of k^{th} air-conditioning load is,

$$T_{ek}(\omega_{rk}, U_i) = \frac{R_{rk}}{s_k}\frac{U_{ek}^2}{(R_{ek} + R_{rk}/s_k)^2 + (X_{ek} + X_{rk})^2} \tag{4}$$

where s_k and U_{ek} are in terms ofω_{rk} and U_i respectively. By the first derivative of (4) equal to 0, the rotor speed ω_{rmaxk} corresponding to the maximum electromagnetic torque is calculated as,

$$\omega_{rmaxk} = \omega_s - \frac{R_{rk}\omega_s}{\sqrt{R_{ek}^2 + (X_{ek} + X_{rk})^2}}. \tag{5}$$

The mechanical torque of air-conditioning load includes the variable part linearly changing with the square of speed and the constant part depending on the friction loss. The mechanical torque of k^{th} air-conditioning load is,

$$T_{mk}(\omega_{rk}) = T_{k0} + \Delta T_k \omega_{rk}^2 \tag{6}$$

where T_{k0} and ΔT_k are the coefficients of constant and variable parts of mechanical torque. The critical starting voltage of k^{th} air-conditioning load can be calculated by $T_{ek}(\omega_{rmaxk},U_i) = T_m(\omega_{rmaxk})$. When there is n controlled air-conditioning loads started up at the same time, the voltage at the connecting point of an aggregator has to meet the starting conditions of all n loads. The critical starting voltage U_{cr} of an aggregator is the minimum voltage meeting the torque balance of air-conditioning loads.

$$U_{cr} = \{\min(U_i)|\ T_{ek}(\omega_{rmaxk}, U_i) \geqslant T_{mk}(\omega_{rmaxk}),\ k \in [1, n]\}. \tag{7}$$

The critical starting voltage of the aggregator of air-conditioning loads can be obtained by (4)(7). To avoid the failure of DLC cycle control, the voltage magnitudes of controlled air conditioners should be greater than or equal to the critical starting voltage at the connecting point of load aggregators. The starting voltage of air-conditioning loads has to be considered as a constraint in DLC cycle control process.

3. Optimal reactive power control model for distribution network with SNOP and DLC

3.1. Objective functions of optimal reactive control model

A load aggregator can shut down or start up the air-conditioning load at the low-voltage side of distribution transformer by remote control devices in the peak load periods to achieve the load-cutting as demand response. In energy markets, the amount of total load-cutting for each participating load aggregators is determined before a day by electric power dispatch centers. As participating load aggregators, they further assign each load reduction to controlled air conditioners by their load-cutting capacities.

There are the following three problems in the load-cutting process of distribution system with SNOP and DLC.

1) The scheduled load-cutting assignment of controlled air conditioners: Different controlled air conditioners are widely connected into different distribution transformer areas. Taking into account, if it is unreasonable for load reduction between controlled air conditioners in different distribution transformers, this feeder may appear reactive power imbalanced problem, which can deteriorate reactive power flowing in a long-distance transmission. Or even worse, it will lead a problem of insufficient starting voltage magnitude of DLC air conditioners. Thus the low-voltage problem is still unable to be solved effectively.
2) The starting voltage requirement of controlled air conditioners: An adequate supply voltage is essential for starting air conditioners. If they have insufficient voltage, those rooms in which air conditioners shut down, will increase room temperatures rapidly. Bad room temperatures have bad influence on consumers directly, which may have load aggregators paid off. To avoid this situation, the voltage magnitudes of controlled air conditioners should be greater than or equal to the critical starting voltage at the connecting point of load aggregators.
3) The deviation between practical and planned active power reduction of air-conditioning loads: Controlled air conditioners play a great role in room temperatures. Due to different room temperatures, it will appear many on/off combinations, which may lead to have a load-cutting deviation problem between practical active power reduction and planned active power reduction. To minimize this deviation as much as possible, the SNOP can be used to regulate the active power transferred between different feeders. Zero deviation between actual reduction and planned reduction by transferring deviation loads to other feeders is available.

It is concluded from the above mentioned, the optimal load-cutting assignments for controlled air-conditioning loads, the optimal control of voltage-adjusting devices and transfer and compensation powers of SNOP are integrated into the proposed model. It is assumed that N_s different controlled air-conditioning loads at the low-voltage side of different distribution transformers are connected into a feeder; Ω_{SNOP} SNOPs connect the feeder to the other feeders. The load reductions of air-conditioning loads are defined as $\Delta P_{D,1}$, $\Delta P_{D,2}$, $\cdots$,$\Delta P_{D,N}$ respectively, as shown in Fig. 5. For the electric power dispatch center, the total amount of planned air-conditioning load reduction is assumed as ΔP_T.

Due to the short lines between distribution transformers and air-conditioning loads, the voltage losses on those lines are negligible. The optimization variables of the proposed model are on/off status of N_s controlled air-conditioning loads and their corresponding load reductions, the active power and reactive power of all SNOP, the reactive power compensation at the low-voltage side of distribution transformers, the reactive power compensation at 110 kV substation and its main transformer ratios. In DLC cycle control process of air-conditioning loads, the low-voltage problem of distribution system can be solved through the effective load reduction and optimal reactive power flow control. Therefore, the three objectives of optimal reactive power flow control are proposed in the proposed model.

1) The sufficient load-cutting of air-conditioning loads eliminate the low-voltage problem in distribution systems. The semi-absolute

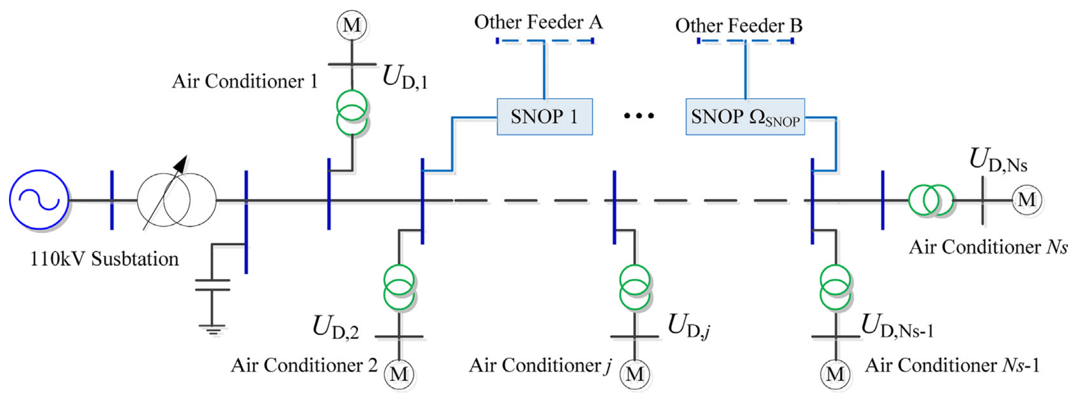

Fig. 5. A 10 kV distribution system with multiple SNOPs and controlled air-conditioning loads.

dispersion [31] is used for indicating low-voltage elimination in the objective as:

$$\min \quad f_1 = \sum_{i=1}^{N_b} \lfloor U_i - U_{i,\min} \rfloor_- \tag{8}$$

where U_i represents the voltage magnitude of bus i, $U_{i,\min}$ is the lower boundary of voltage magnitude of bus i, N_b is the number of buses in the 10 kV distribution system, and $\lfloor v \rfloor_-$ represents $v = max\{0, -v\}$, for any real number v.

2) The on/off status μj of a controlled air-conditioning load j is determined by both room temperatures and the limit temperatures of cycle control.

$$\mu_j = \begin{cases} 1, & T_{j,\min} \leqslant T_j \leqslant T_{j,\max} \\ 0, & T_j \geqslant T_{j,\max} \end{cases} \tag{9}$$

where μ_j represents the controlled state of the controlled air-conditioning load j, which $\mu_j = 1$ indicates that the air-conditioning load j is shut down; on the contrary, $\mu_j = 0$ indicates that the air-conditioning load j is switched on. T_j represents the room temperature of the air-conditioning load j. $T_{j,\min}$ and $T_{j,\max}$ are the minimum and maximum critical temperatures for the air-conditioning load j in the DLC cycle control, respectively.

A number of controlled air conditioners are switched on, when room temperatures are higher than $T_{j,\max}$. This causes a large load increase in distribution systems, and perhaps leads to the low-voltage problem again. In order to avoid the low-voltage problem once again, there will be extending time periods of air conditioners that are turned off, even though the room temperature of controlled air-conditioning load j is higher than $T_{j,\max}$. This is

$$\mu_j = 1, \quad T_j \geqslant T_{j,\max}. \tag{10}$$

However, room temperatures are continuing to be raised and extended, if air conditioners are turned off, which causes bad influence on the comfort of users. Thus, the objective function of minimizing deviation between the controlled state and the ideal state of controlled air-conditioning load j, which is used to eliminate the negative effect on the comfort of users.

$$\min \quad f_2 = \sum_{j=1}^{N_s} (\mu_j - \mu_j^*)^2 \tag{11}$$

where μ_j^* represents the ideal control state of controlled air-conditioning load j satisfying (9); μ_j represents the practical control state of controlled air conditioners.

3) To maximum the economic benefits of distribution system, the active power losses of the distribution network and the SNOP should be as small as possible.

$$\min \quad f_3 = P_{Loss,NET} + \sum_{l=1}^{\Omega_{SNOP}} P_{Loss,SNOP}^{l} \tag{12}$$

where $P_{Loss,NET}$ is the active power loss of the network; $P_{Loss,SNOP}^{l}$ is the active power loss of l^{th} SNOP, which is made up of the losses of semiconductors, passive components and the cooling system. The $P_{Loss,SNOP}^{l}$ is divided into three components: no load loss, linear loss and quadratic loss depending on the converter current [17], so that it can be measured in terms of the apparent power of the converter. The $P_{Loss,SNOP}^{l}$ can be obtained as,

$$P_{Loss,SNOP}^{l} = aS_{SNOP}^{l} + b\sqrt{S_{SNOP}^{l}} + P_{L0,SNOP}^{l} \tag{13}$$

where S_{SNOP}^{l} represents the apparent power of l^{th} SNOP; a and b are the coefficients of the active power loss; $P_{L0,SNOP}^{l}$ represents the fixed loss of l^{th} SNOP. It is noted that a SNOP contains two VSCs sharing a DC link, so that the active power loss of a SNOP is the sum of the power losses of these two VSCs, and the power loss of each VSC can be calculated by (13). In the above three objective functions, we consider the low-voltage problem-solving objective is as the priority, which is for keeping security operation of distribution systems; and then minimizing negative impacts on the comfort of users as much as possible in the DLC cycle control, and ensuring demand response working effectively in the long-term; at last, the economic benefits of distribution system is finally considered.

3.2. Constraints of optimal reactive control model

The constraints of the model include the network power flow constraints, the operation constraints of conventional reactive power compensation and main transformer ratio, and the operation constraints of controlled air-conditioning loads and SNOPs. The operation constraints of controlled air-conditioning loads should take the critical starting voltage into consideration, which is the voltage magnitude $U_{D,j}$ greater than or equal to the critical starting voltage $U_{cr,j}$ at the connecting point of aggregators. The operation constraints for air-conditioning loads are,

$$\begin{cases} \underline{\Delta P_{D,j}} \leqslant \mu_j \Delta P_{D,j} \leqslant \overline{\Delta P_{D,j}} \\ \Delta Q_{D,j} = \Delta P_{D,j} \cdot \tan\gamma \\ U_{cr,j} \leqslant U_{D,j} \\ \mu_j \in \{0, 1\} \end{cases} \quad j = 1, \ldots N_s \tag{14}$$

where $U_{cr,j}$ represents the critical starting voltage of the controlled air-conditioning load j obtained by (7); tanγ is the power factor of air-conditioning load, $\underline{\Delta P_{D,j}}$ and $\overline{\Delta P_{D,j}}$ are the minimum and maximum reduction of controlled air-conditioning load j.

Fig. 6 shows that two distribution feeders are connected through a SNOP composed of VSCi and VSCj sharing a DC link. The SNOP can accurately control the transfer active power through two feeders, while

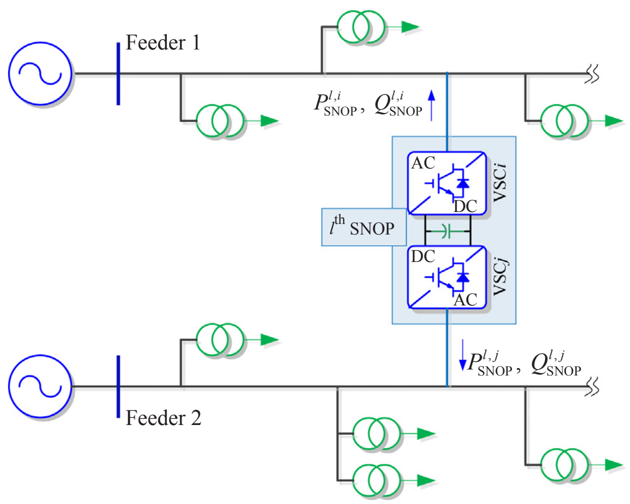

Fig. 6. Two distribution feeders connected by a SNOP.

provide reactive power compensation supporting for those two feeders as well. For l^{th} SNOP in Fig. 6, $P^{l,i}_{\mathrm{SNOP}}$ and $Q^{l,i}_{\mathrm{SNOP}}$ are the active and reactive powers of VSCi injecting into feeder 1, and $P^{l,j}_{\mathrm{SNOP}}$ and $Q^{l,j}_{\mathrm{SNOP}}$ are the active and reactive powers of VSCj injecting into feeder 2. The reactive power adjustments of VSCs are independent, while their active powers need to meet the conservation of energy. That is the sum of active powers of VSCs and the active power loss of SNOP is equal to zero. To consider the power loss of the SNOP, the active power transfer constraint of l^{th} SNOP is,

$$P^{l,i}_{\mathrm{SNOP}} + P^{l,j}_{SNOP} + P^{l}_{Loss,SNOP} = 0 \quad l \in \Omega_{SNOP} \tag{15}$$

where Ω_{SNOP} is the SNOP set; $P^{l}_{Loss,SNOP} = P^{l,i}_{Loss,SNOP} + P^{l,j}_{Loss,SNOP}$ is the power loss of l^{th} SNOP, which is the sum of the power losses of VSCi and VSCj, and $P^{l,i}_{Loss,SNOP}$ and $P^{l,j}_{Loss,SNOP}$ can be calculated by (13). The reactive power injected constraints is,

$$\begin{cases} Q^{l,i}_{SNOP,\min} \leqslant Q^{l,i}_{SNOP} \leqslant Q^{l,i}_{SNOP,\max} & l \in \Omega_{SNOP} \\ Q^{l,j}_{SNOP,\min} \leqslant Q^{l,j}_{SNOP} \leqslant Q^{l,j}_{SNOP,\max} & l \in \Omega_{SNOP} \end{cases} \tag{16}$$

where $Q^{k,i}_{SNOP,\min}$, $Q^{k,j}_{SNOP,\min}$ and $Q^{k,i}_{SNOP,\max}$, $Q^{k,j}_{SNOP,\max}$ are the lower and upper limits of the reactive power of two VSCs in l^{th} SNOP. And the apparent power of VSCs cannot exceed the rated capacity. The SNOP capacity constraint is,

$$\begin{cases} \sqrt{P^{l,i^2}_{SNOP} + Q^{l,i^2}_{SNOP}} \leqslant S^{l,i}_{SNOP} & l \in \Omega_{SNOP} \\ \sqrt{P^{l,j^2}_{SNOP} + Q^{l,j^2}_{SNOP}} \leqslant S^{l,j}_{SNOP} & l \in \Omega_{SNOP} \end{cases} \tag{17}$$

where $S^{k,i}_{SNOP}$ and $S^{k,j}_{SNOP}$ are the rated capacities of two VSCs in l^{th} SNOP. The active power transfer and reactive power compensation of SNOP are applied to support the voltage control of the network with air-conditioning loads.

Since SNOPs regulate the transfer active power between two feeders, the practical load reduction can be equal to the planned load reduction. Thus, the operation constraints of SNOP are composed of (8) (10), and the active power balance constraint as follows:

$$\sum_{j=1}^{N_s} \mu_j \Delta P_{D,j} - \Delta P_T + P^{k}_{\mathrm{SNOP}} = 0 \quad k \in \Omega_{SNOP}. \tag{18}$$

The constraints of the proposed model contain the nonlinear power flow equations and the 0–1 on/off status of controlled air conditioners. This model is a mixed nonlinear integer with multi-objective programming problem. Since the model optimization variable is 0–1 integer variables and continuous variables, we can take 0–1 integer variables as a population, and continuous variables as a population. A parallel cooperative co-evolutionary differential evolution algorithm [32] is used to solve the model due to the better solution efficiency.

4. Case study

A practical 10 kV distribution system contains 54 buses shown in Fig. 7. A 110 kV substation has been installed reactive power

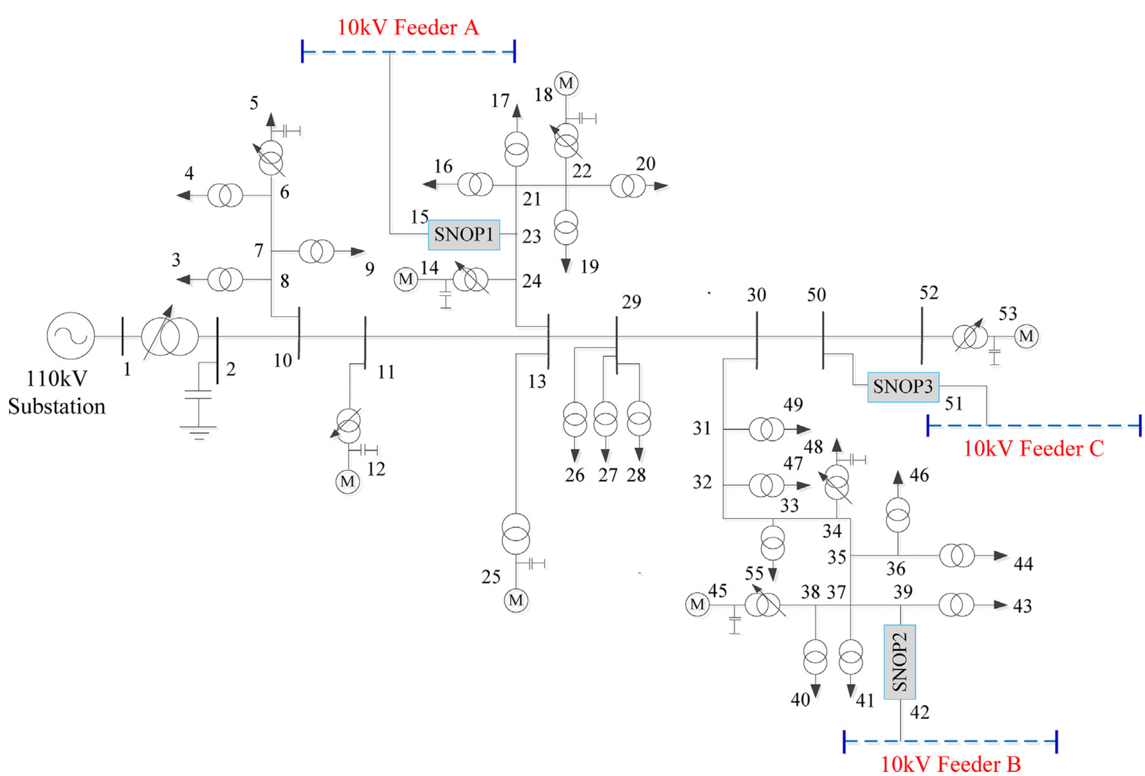

Fig. 7. A 54-bus distribution system.

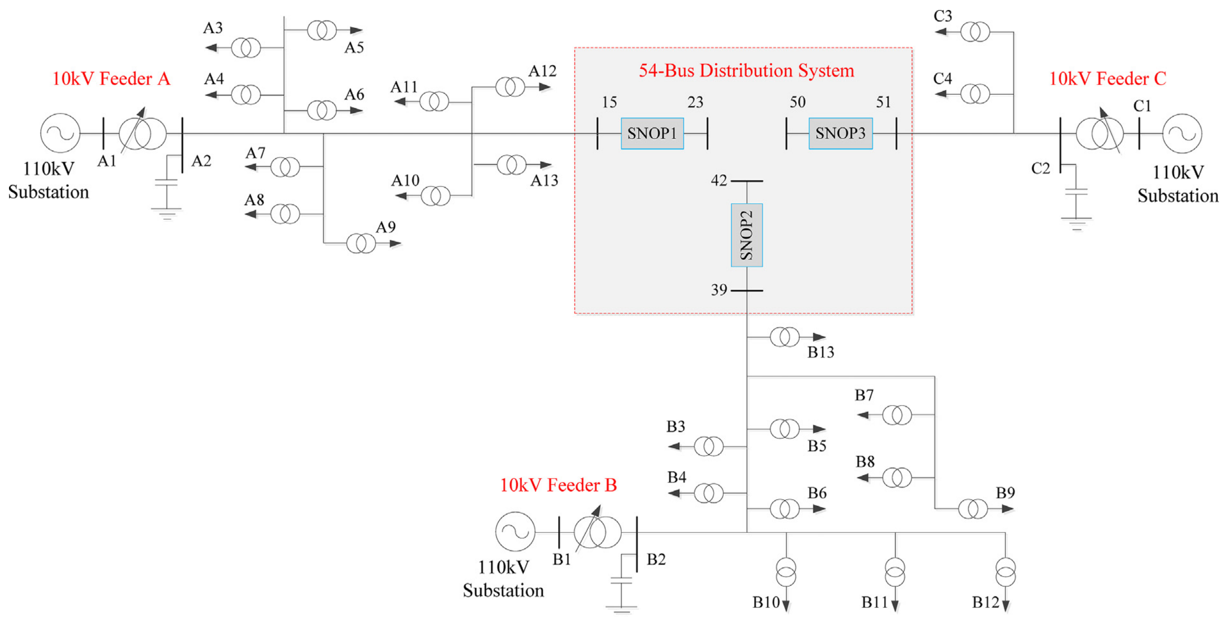

Fig. 8. Distribution networks of 10 kV Feeders A, B and C.

Table 1
Initial parameters of air-conditioning load.

Connected bus	Initial status μ_0	Initial remperature/°C	Load reduction/kW
4	On	26.0	68
12	On	25.1	68
14	On	27.4	54
18	On	28.3	38
25	On	28.2	34
45	On	28.5	54
53	On	29.4	36

compensation capacitors buses of 2, 5, 13, 15, 19, 26, 46, 49 and 54. The basic power is 100 kVA and basic voltage is 10 kV. Bus 1 is the swing bus of system. There are SNOP1, SNOP2 and SNOP3 with capacities of 1000, 800 and 1500 kVA respectively; 7 air-conditioning loads connected to bus 4, 12, 14, 18, 25, 45 and 53 managed by the load aggregator. The three SNOPs connect the 54-bus distribution system to the feeders A, B and C respectively, and the networks of feeders A, B and C are shown in Fig. 8. The coefficients a and b of the active power loss of SNOP1, SNOP2 and SNOP3 are 0.02 and 0.01, 0.016 and 0.08, 0.03 and 0.02, respectively. It is assumed the room temperatures are within [26 °C, 28 °C]. The critical starting voltages of load aggregator are about 226 V, which is 0.97pu. The parameters of air-conditioning loads are seen in Table 1, and the time-varying temperature equation is used to calculate the temperature [9]. The load data and room temperatures are from SCADA and remote sensors of air conditioners in Chengdu, China. The data are from 12:00 am to 13:00 pm with 5 min as intervals on 21th, July 2016. The scheduled load-cutting time between the dispatching center and the load aggregator is 12: 00–13: 00 with an amount of 224 kW load-cutting. The voltage allowable range is from 0.9 pu to 1.07 pu. The results of initial flow and optimal flow solution during the cycle control period of 12:00 and 13:00 are compared.

4.1. Comparison of low-voltage control effects

Fig. 9 shows the voltages for 54-bus power distribution system obtaining by the power flow at the initial status of air-conditioning loads and the initial room temperatures of Table 1. In Fig. 9, the ideal voltages after DLC control of [9] indicate that the voltage magnitudes with ideal DLC load-cutting, in this extreme case that all air-conditioning

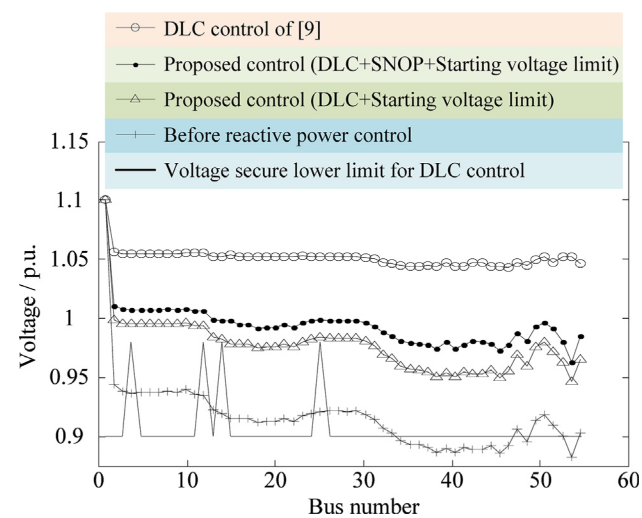

Fig. 9. Comparison of bus voltages for 54-bus distribution system.

loads are cut off, and the air-conditioning load reduction reaches the maximum amount. And the DLC control of [9] cannot determine whether the cutting air-conditioning loads can be started up in the next control cycle. The lower boundary of voltage security is the composed by the critical starting voltage magnitudes constraints and the voltage security constraints. The critical starting voltage magnitudes constraints are determined by practical states in the 1st time-period shown in Table 2. And additionally, Table 2 gives ideal control status of all controlled air conditioners.

The room temperatures of air conditioners in bus 4, bus 12 and bus 14 we given from Table 1 are below 29°, thus DLC cycle control turns these air conditioners off. For air conditioners in bus 25, although it is above 28°, that they are switched off as well in DLC cycle control. In order to have controlled air conditioners that are switched off to get started, sufficient voltage magnitudes of those 4 buses are greater than or equal to the critical starting voltage magnitude 0.97 p.u. It is assume that if all of controlled air conditioners are switched off after DLC cycle control, total system loads are the minimum and ideal voltage magnitudes are seen as the curve after DLC control of [9] in Fig. 9. The feasible voltages of the proposed control method are between the curve

Table 2
Control status of air-conditioning load.

Connected bus	Initial temperature/ °C	Ideal control status μ^*	Practical control status μ
4	26.0	Off	Off
12	25.1	Off	Off
14	27.4	Off	Off
18	28.3	On	On
25	28.2	On	Off
45	28.5	On	On
53	29.4	On	On

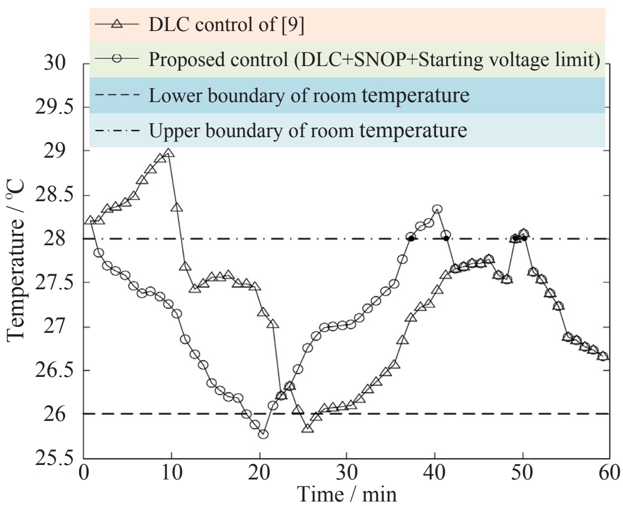

Fig. 10. Comparison of room temperatures at bus 25.

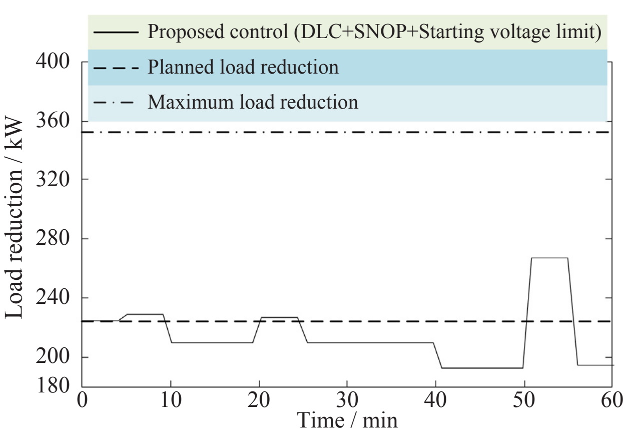

Fig. 11. Load-cutting curves of controlled air conditioners.

after DLC control and the curve before the reactive power control.

In Fig. 9, the voltages of bus 34–46, 48, 52 and 53 are below the voltage security constraints. There are existing serious low-voltage problems in bus 40– bus 46, bus 48, bus 53 which are load buses of distribution transformer. But, they are not appearing any low-voltage problems after the proposed control methods, and critical starting voltage magnitudes constraints at bus 4, 12, 14 and 25 are satisfied as well. Comparing the voltages by the proposed control methods with and without SNOP, the voltage magnitudes at bus 12 and bus 14 are above critical starting voltage magnitude about 0.015–0.02 when the SNOPs are not connected into distribution system after DLC cycle control. It also has a possibility of DLC control failures if the consuming loads are further increasing in a rapid speed. But for 10 kV distribution system with SNOP, all voltage magnitudes at each bus are higher than voltage magnitudes in distribution system without SNOP. It can be seen that the

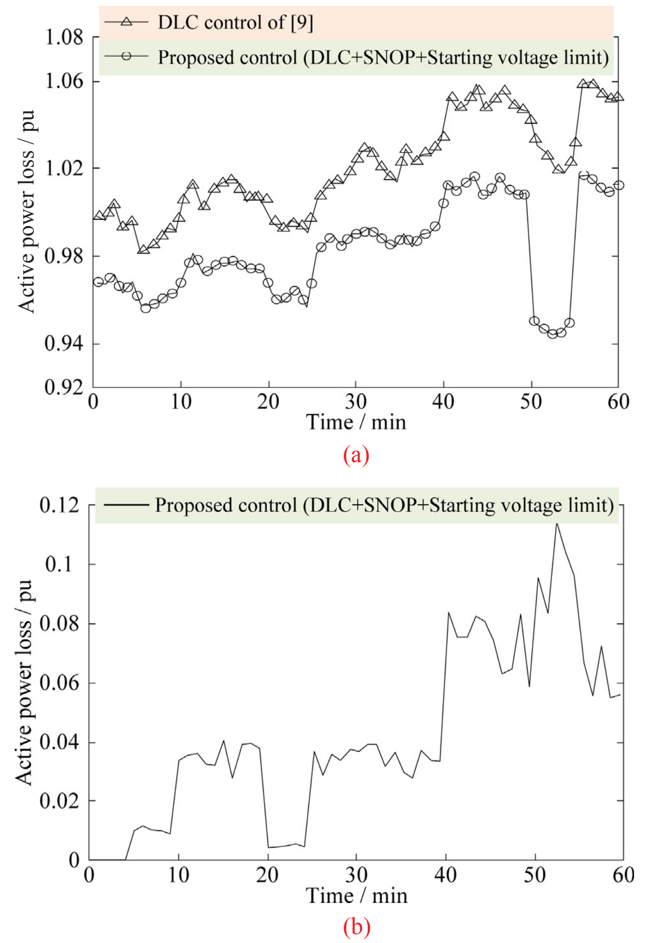

Fig. 12. Active power losses of the distribution system: (a) Active power loss of network, (b) Active power loss of SNOP.

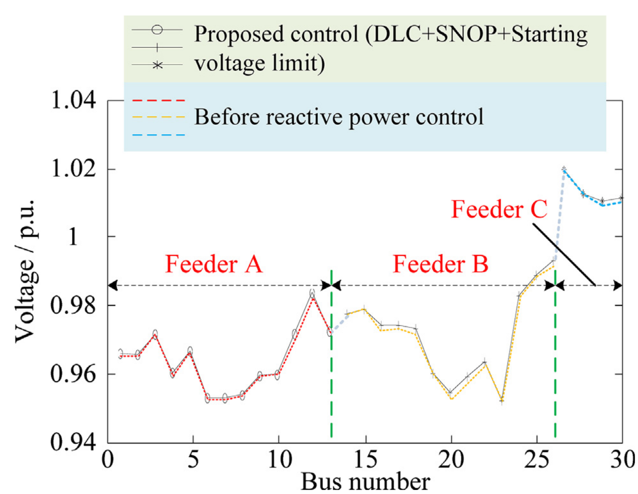

Fig. 13. Voltage changes of 10 kV Feeders A, B and C caused by SNOP.

DLC control can continue to working, even though consuming loads are further increasing in a rapid speed. It is greatly effective for DLC air-conditioning cycle control and low-voltage control if SNOP are connected into distribution systems. Fig. 10 shows the room temperatures in the DLC cycle control between 0 and 60 min at bus 25. It can be seen that the room temperature obtained by the DLC control of [9] increases from 28.2 °C to 29.03 °C, then decrease to about 25.8 °C. The room temperature are better controlled by the proposed control method, and the corresponding room temperatures are basically controlled in [26 °C, 28 °C], which never lower than 25.5 °C, or higher than 28.5 °C. This finding implies that the 2nd objective function of minimizing deviation is working, which can maintain the load-cutting is satisfied to the comfort requirements of customer.

4.2. Comparison of load cutting and power loss

Fig. 11 shows the load-cutting curves of air conditioners for this 10 kV distribution system. The total amount of load reduction of controlled air conditioners is closed to the planned load-cutting by electric power dispatching center. The minimum deviation is 0, and the maximum positive deviation is 40 kW and negative deviation is 30 kW respectively. This is because room temperatures of controlled air conditioners are different, which causes practical control pattern may differ from ideal control pattern, which means appearing load-cutting deviation.

For the active power transferred by SNOP, a load-cutting deviation between practical reduction and planned reduction is eliminated by SNOP transmission. For example, the practical load reduction is 40 kW, which is greater than planned reduction in the time-period of 50–55 min. Three SNOP are injected active power from other feeders into this distribution system by 12 kW, 20 kW, 8 kW, which are equal to 40 kW in total referred to load reduction deviation. Fig. 12 shows the curves of active power loss in this distribution system by the DLC control of [9] and the proposed method. The results by the proposed method include the active power losses of the network and the SNOP. The active power loss of the network with DLC and SNOP is obviously smaller than that without SNOP. This finding shows that the SNOP are reducing active power loss, and improving the economic benefits of distribution system operation.

The active power loss of three SNOPs is shown in Fig. 12(b), which has a positive relationship with the transferred power flow of SNOPs. It is known that the load-cutting deviation between practical reduction and planned reduction is eliminated by active power transferred by SNOPs. Therefore, the corresponding total active power losses of these three SNOPs are varied with the load-cutting deviation. Compared with Fig. 12(a), these losses are quite smaller than network losses, so that the 3rd objective function is mainly dealing with how to decrease network losses.

The SNOPs need to transfer the maximum active power at 55 min for this 54-bus distribution system in Fig. 11. To analyze the effects of SNOP on the other feeders, Fig. 13 shows the voltage magnitudes of 10 kV feeders A, B and C at 55 min before and after the implementation of the proposed control method. In Fig. 13, the voltage magnitudes are all in the secure ranges of [0.95 p.u., 1.05 p.u.] before and after the proposed reactive power control, and there are slight impacts on the voltage of feeders A, B and C caused by the SNOPs. This is because the transferred active power flow of feeder A, B and C brought by SNOPs is used for eliminating the load-cutting deviation, which is essentially not very large. And the SNOPs can also provide the reactive power compensation for helping voltage magnitudes maintain in a steady range. Thus, the proposed control method has limited effects on the voltage magnitudes of the other feeders.

5. Conclusions

This paper presents an optimal reactive power control method for distribution systems with SNOP and DLC air-conditioning loads. The air-conditioning starting voltage constraints for the connecting point to distribution systems of load aggregators is studied based on the DLC cycle control and the characteristics of starting voltage. This can provide the formula for calculating the critical starting voltage of air-conditioning loads. We take full advantage of SNOP with reactive power compensation characteristics, and eliminate load-cutting deviation between planned load reduction and practical load reduction. This realizes to accurate DLC cycle control for load-cutting, and help electric power dispatch center rapidly shifts and avert power scheduling for peak loads in effective way. We combine demand response technology and voltage control as a comprehensive method to deal with the low-voltage problem at the overload condition of distribution systems. It provides an effective and reasonable approach for demand-side management of smart distribution systems.

Acknowledgments

This work was supported by the National Natural Science Foundation of China (51607015), Chongqing Research Program of Basic Research and Frontier Technology (cstc2016jcyjA0402) and Fundamental Research Funds for the Central Universities (106112016CDJXY150001).

Appendix A. Supplementary data

Supplementary data associated with this article can be found, in the online version, at http://dx.doi.org/10.1016/j.ijepes.2018.06.027.

Reference

[1] Chen P, Salcedo R, Zhu Q, de León F, Czarkowski D, Jiang ZP, et al. Analysis of voltage profile problems due to the penetration of distributed generation in low-voltage secondary distribution networks. IEEE Trans Power Del 2012;27(4):2020–8.
[2] Zhang W, Lian J, Chang C, Kalsi K. Aggregated modeling and control of air conditioning loads for demand response. IEEE Trans Power Syst 2013;28(4):4655–64.
[3] Meyn S, Barooah P, Busic A, Chen Y, Ehren J. Ancillary service to the grid using intelligent deferrable loads. IEEE Trans Autom Control 2015;60(11):2847–62.
[4] Haider HT, See OH, Elmenreich W. A review of residential demand response of smart grid. Renew Sustain Energy Rev 2016;59:166–78.
[5] Gutiérrez-Alcaraz G, Tovar-Hernández JH, Lu CN. Effects of demand response programs on distribution system operation. Electr Power Energy Syst 2016;74:230–7.
[6] Hu B, Wang H, Yao S. Optimal economic operation of isolated community microgrid incorporating temperature controlling devices. Protect. Control Modern Power Syst. 2017;2(1):6.
[7] Dorahaki S, Rashidinejad M, Abdollahi A, Mollahassani-pour M. A novel two-stage structure for coordination of energy efficiency and demand response in the smart grid environment. Electr Power Energy Syst 2018;97:353–62.
[8] Shad M, Momeni A, Errouissi R, Diduch CP, Kaye ME, Chang L. Identification and estimation for electric water heaters in direct load control programs. IEEE Trans Smart Grid 2017;8(2):947–55.
[9] Lu N. An evaluation of the HVAC load potential for providing load balancing service. IEEE Trans Smart Grid 2012;3(3):1263–70.
[10] Bashash S, Fathy H. Modeling and control of aggregate air conditioning loads for robust renewable power management. IEEE Trans Control Syst Technol 2013;21(4):1318–27.
[11] Liu M, Shi Y. Model predictive control of aggregated heterogeneous second-order thermostatically controlled loads for ancillary services. IEEE Trans Power Syst 2016;31(3):1963–71.
[12] Chen X, Yi Y, Zhang Y, Li Q, Zhu J, Cai Z. Approach to setting gateway reactive power control band for distribution networks with wind power. IET Gener Transm Distrib 2017;11(3):596–604.
[13] Samimi A, Nikzad M. Complete active-reactive power resource scheduling of smart distribution system with high penetration of distributed energy resources. J Mod Power Syst Clean Energy 2017;5(6):863–75.
[14] J. Bloemink, and T. Green, "Increasing photovoltaic penetration with local energy storage and soft normally-open points", in 2011 IEEE PES general meeting, vol. 1, pp. 1–8, 2011.
[15] Bloemink J, Green T. Benefits of distribution-level power electronics for supporting distributed generation growth. IEEE Trans Power Del Apr. 2013;28(2):911–9.
[16] Cao W, Wu J, Jenkins N, Wang C, Green T. Operating principle of soft open points for electrical distribution network operation. Appl Energy 2016;164:245–57.
[17] Cao W, Wu J, Jenkins N, Wang C, Green T. Benefits analysis of soft open points for electrical distribution network operation. Appl Energy 2016;165:36–47.
[18] Wang C, Song G, Li P, Ji H, Zhao J, Wu J. Optimal siting and sizing of soft open points in active electrical distribution networks. Appl Energy 2017;189:301–9.
[19] Long C, Wu J, Thomas L, Jenkins N. Optimal operation of soft open points in medium voltage electrical distribution networks with distributed generation. Appl Energy 2016;184:427–37.
[20] Xing X, Lin J, Wan C, Song Y. Model predictive control of LPC-looped active distribution network with high penetration of distributed generation. IEEE Trans. Sustain. Energy 2017;8(3):1051–63.
[21] P. Li, H. Ji, C. Wang, J. Zhao, G. Song, F. Ding, and J. Wu, "Optimal operation of soft open points in active distribution networks under three-phase unbalanced conditions", IEEE Trans. Smart Grid, in press.
[22] Falahi M, Butler-Purry K, Ehsani M. Induction motor starting in islanded

microgrids. IEEE Trans Smart Grid 2013;4(3):1323–31.

[23] Wang X, Yong J, Xu W, Freitas W. Practical power quality charts for motor starting assessment. IEEE Trans Power Del Apr. 2011;26(2):799–808.

[24] Liu M, Shi Y, Liu X. Distributed MPC of aggregated heterogeneous thermostatically controlled loads in smart grid. IEEE Trans Ind Electron 2016;63(2):1120–9.

[25] Bhattarai BP, Myers KS, Bak-Jensen B, de Mendaza ID, Turk RJ, Gentle JP. Optimum aggregation of geographically distributed flexible resources in strategic smart-grid/microgrid locations. Electr Power Energy Syst 2017;92:193–201.

[26] Huang X, Yang Y, Taylor GA. Service restoration of distribution systems under distributed generation scenarios. CSEE J Power Energy Syst 2016;2(3):43–50.

[27] Paterakis NG, Erdinc O, Bakirtzis AG, Catalao JPS. Load-following reserves procurement considering flexible demand-side resources under high wind power penetration. IEEE Trans Power Syst 2015;30(3):1337–50.

[28] L. Latchoomun and D. Sooben, “A low cost automated scheme to avoid load shedding during simultaneous start-up of single and three-phase aplit air-conditioning units”, 2012 2nd Int. Symp. Environ. Friendly Energies Appl., EFEA, Newcastle upon Tyne, 2012, pp. 207–211.

[29] Zhou N, Wang P, Wang Q, Loh PC. Transient stability study of distributed induction generators using an improved steady-state equivalent circuit method. IEEE Trans Power Syst 2014;29(2):608–16.

[30] Wang XF, Song YH, Irving M. Modern Power Systems Analysis. Berlin, Germany: Springer; 2008.

[31] Konno H, Koshizuka C. Mean-absolute deviation model. IIE Trans 2005;37(10):893–900.

[32] Liang C, Chung C, Wong K, Duan X. Parallel optimal reactive power flow based on cooperative co-evolutionary differential evolution and power system decomposition. IEEE Trans Power Syst 2007;22(1):319–23.